Submillimeter-wave waveguide filters fabricated by SU-8 process and laser micromachining

Shang, Xiaobang; Yang, Hao; Glynn, David; Lancaster, Michael

DOI:
10.1049/iet-map.2016.0951

Document Version
Peer reviewed version

Citation for published version (Harvard):
Shang, X, Yang, H, Glynn, D & Lancaster, M 2017, 'Submillimeter-wave waveguide filters fabricated by SU-8 process and laser micromachining', *IET Microwaves, Antennas and Propagation*. https://doi.org/10.1049/iet-map.2016.0951

Submillimeter wave waveguide filters fabricated by SU-8 process and laser micromachining (Review paper)

Xiaobang Shang*, Hao Yang, David Glynn, Michael J. Lancaster

Department of Electronic Electrical and Systems Engineering, the University of Birmingham, B15 2TT, Birmingham, United Kingdom
*shangxiaobang@gmail.com

Abstract: For terahertz systems, rectangular waveguide is an ideal low loss medium for interconnectivity and the construction of passive circuits. A drawback when manufacturing waveguides at submillimeter wavelengths is the demanding tolerances due to small dimensions. For example a WR-3 waveguide (operating between 220 and 325 GHz) has a cross-sectional dimension of just 864 by 432 μm, and higher frequency waveguides get proportionally smaller. An additional challenge is that if using waveguide for passive circuits such as filters, there are additional structures inside the waveguide which are significantly smaller than the waveguide itself. Traditionally, computer numerical control (CNC) milling has been used for waveguides, however at terahertz frequencies this is difficult to utilise. In this paper emerging technologies for terahertz waveguides are compared with conventional CNC solutions. The technologies include the photo-lithography based polymer etching of waveguides using SU-8 photoresist, and the laser machining of metal. Both have shown promise, and good quality terahertz passive components have been fabricated and measured.

1. Introduction

Waveguide is a type of transmission line, usually in the form of a rectangular metal tube. Compared with other common transmission line types operating at the same frequencies, waveguide exhibits the lowest loss and the best power handling capacity, but suffers from the drawback of bulky size. When operating at frequencies such as W-band and beyond, waveguide becomes more and more popular, mainly due to its low loss characteristics. However, with rising frequencies, the size of the waveguide decreases and the tolerances on dimensions become tighter; both of which bring challenges for fabrication methods. Waveguide filters based on coupled resonators are a particular challenge because their resonant frequencies are sensitive to dimensional inaccuracy, and unloaded quality factors are dependent upon surface integrity. Researchers have been actively studying this and different manufacturing techniques have been proposed to accommodate the fabrication of complex waveguide features. This paper is devoted to reviewing the current state of these techniques as well as the waveguide filters operating in the frequencies from W-band and beyond.

Computer numerically controlled (CNC) machining is widely utilised for the production of metal waveguide components at submillimeter wave frequencies, usually using a split-block technique. This requires the waveguide to be split along the middle of the waveguide broadside wall for minimized loss due to no surface current flowing across the joints. CNC machining together with the split-block technique is the main competitor to micromachining techniques. Researchers have been pushing the limit of conventional CNC machining, with milled waveguide filters demonstrated at W-band [1-2], WR-6 band [3] and WR-3 band [4]. Beyond this frequency, CNC machining is struggling to overcome the challenges of available cutter sizes, the wear and breakage of cutters, generation of defects/recesses and cracks due to mechanical stresses, and achievable aspect ratios [5-6]. To accommodate the fabrication of complex terahertz waveguide circuits, improvements are being made with CNC machining; an example of a purpose-built ultra-high precision CNC micromachining platform is developed and reported in [7]. This reflects where the current state-of-the-art of CNC machining lies, with typical dimensional accuracies of 2-3 μm, a surface roughness Ra of 75 *n*m, a smallest tool diameter of 25 μm and aspect ratios greater than 5:1. A range of waveguide circuits covering W-band to 2.7 THz are successfully demonstrated using this platform [7]. It is worth pointing out that CNC machines with such tight tolerance are very expensive and not readily available.

Metal electroforming over a photoresist mould is another viable way to obtain an all-metal waveguide structure at terahertz frequencies. For this technique, the mould is usually produced from photoresist using a lithography process, and therefore good accuracy is transferred to the formed metals. An electroformed all copper waveguide structure with a dimensional accuracy of around 1 μm and a RMS surface roughness of around 300 *n*m is reported in [8]. An all-copper waveguide branch coupler, for frequencies as high as 1.3 THz, has been demonstrated using micro-electroforming with an SU-8 mould [9]. High frequency waveguide filters fabricated by electroforming have not been reported in open literature yet.

Additive manufacturing (also known as 3-D printing) is another very promising technique to produce high frequency waveguide devices. There are many advantages when using 3-D printing for microwave applications. One of these advantages is the potential weight reduction by using plated polymer materials, where not only is the density of the material reduced compared to pure copper, but the filter can also be shaped appropriately to reduce its mass. This includes removing material at current nulls in the resonator structure [5]. A second advantage is the enhancement in performance. Because 3-D printing enables designs with geometrical complexity, filters can be easily

constructed from novel shapes such as spherical resonators which have ultra-high unloaded quality factors [10]. Three different 3-D printing techniques, namely fused deposition modelling, stereolighography apparatus (SLA) and selective laser sintering (SLS), have found the most application in the fabrication of waveguide structures. Presently, SLA process offers the highest resolution and the best surface integrity [11]. The state-of-the-art SLA process provides a dimensional accuracy of 25 μm and a surface roughness of around 1 μm [12]. Such precision enables the successful implementation of waveguide filters, with the highest reported frequencies up to W-band [5, 11]. The SLS process allows all-metal waveguide structures to be produced, at the penalty of degraded dimensional accuracy and increased surface roughness. Two E-band (60-90 GHz) waveguide iris coupled filters printed from $CuSn_{15}$ alloy powder using the SLS technique are reported in [13]. Although both filters are comprised of a large number of resonators (>10), they have an acceptable measured performance with relatively small deviation in responses between simulation and measurement. The deviation is mainly attributed to (i) significant surface roughness which is measured to be 6 μm; and (ii) shrinkage of dimensions which is estimated to be in the range of 2-3% [13]. These two filters are currently the highest frequency waveguide filters implemented by the SLS process. Note that both SLA and SLS techniques are relatively new and their tolerances are expected to improve significantly over time, with potential for 3-D printed waveguide filters to be demonstrated in the terahertz region soon.

Silicon deep reactive-ion etching (DRIE) of bulk silicon wafers is another feasible and attractive technique for fabrication of terahertz waveguide structures. The DRIE process has been utilised to demonstrate waveguide filters across a wide range of frequencies, including W-band [14], WR-2.2 band [15-16], WR-1.5 band [17-18], and WR-1 band [19]. This lithography based process is ideally suited for large size batch production, and is capable of offering uniformity between batches. Different to CNC machining, DRIE can cope with the smaller size and better accuracy with increasing frequencies and becomes more competitive in terms of shorter production time [19]. However, the etching based DRIE process suffers from three main problems, i.e. difficulties to maintain straight sidewalls and achieve uniform depth across the wafer for each etch depth, and relatively poor surface roughness on the sidewalls [20-21]. These problems can be addressed to a certain extent by more complex process development [20]. For a well-established DRIE process, the typical tolerance on dimensions is 2 μm, with a sidewall angle of up to 3° [18]. Note that these tolerances vary with wafer thickness. Reference [19] reports an improved etching angle as low as 0.5°, measured on a WR-1 waveguide filter. This filter also has an excellent reported surface roughness of 100 *n*m [19]. Usually, waveguide circuits are formed from two etched silicon pieces and within each piece only features of the same depth are allowed. Recently, a further advancement on the technique is reported in [22], which describes a multistep DRIE process allowing multi-depth waveguide features with ±2% tolerance. This additional flexibility allows more complex waveguide devices to be constructed and enables the possibility of integration of multiple components onto a single silicon package.

Polymer based micro hot embossing, coupled with selective electroplating, is a desirable replication process for large scale production of waveguide components. Low-cost and low weight are the two principle advantages of this technique. Micro hot embossing also opens up the possibility of easy and fully integration of waveguide components in a communication system, and yields a significant cost saving on packaging. A W-band filter using this technique is reported in [23]. The measurement performance is not ideal and this is attributed to the inaccuracy of the mould, as well as significant shrinkage of the plastic (< 4%) [23]. This work implies that the micro hot embossing technique is not yet mature enough for the production of high frequency waveguide components.

2. SU-8 micromachining

SU-8 micromachining, is a photolithographic based process and is another feasible solution to fabricate millimetre-wave and terahertz waveguide components. SU-8 is capable of constructing three dimensional terahertz waveguide structures with high aspect ratios (greater than 20:1), high dimensional accuracy (tolerance within a few microns), and excellent surface integrity (roughness on the order of tens of nanometres) [24]. The SU-8 process has been utilised to demonstrate a range of millimetre-wave and terahertz circuits, including filters [21, 25-28], waveguides [29-30], Butler matrix with a patch antenna array [31], an orthomode transducer [32], and antennas [33-35].

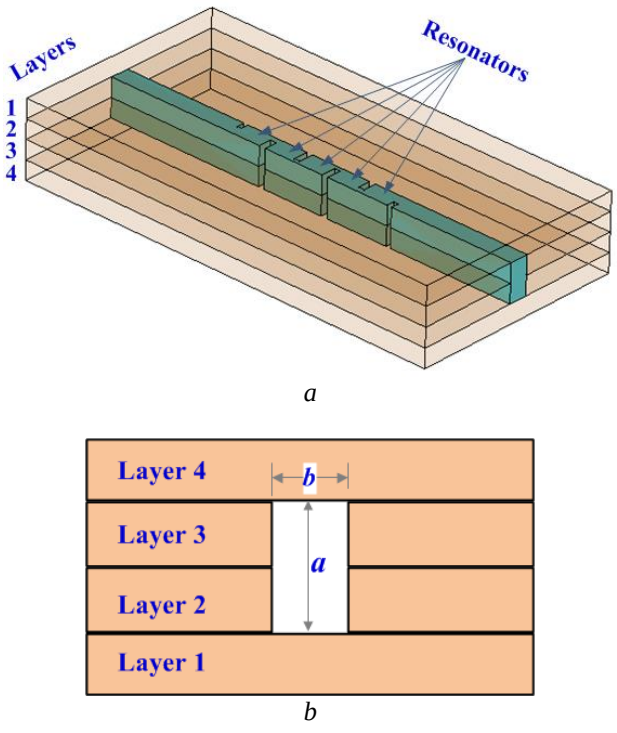

Fig. 1. *WR-3 waveguide filter consisting of four SU-8 layers with the same thickness of 432 µm.* [21]
(a) Illustration of the waveguide filter structure. The turquoise part in the middle of the structure is the hollow channel.
(b) A cross-sectional view from either end of the filter. *a*=864 μm, *b*=432 μm.

In comparison with conventional CNC machining, the SU-8 process has advantages in terms of (i) low cost for large size batch production and high uniformity within and between batches; (ii) high dimensional accuracy provided by photolithography process; (iii) small surface roughness (<40 *n*m) on sidewalls; and (iv) easy replication of complex shapes and/or large format arrays due to patterning without additional cost. The SU-8 process is capable of achieving comparable dimensional accuracy to DRIE, with a much lower capital investment on equipment as well as a better surface integrity on sidewalls.

As an example of the SU-8 process in the following sections, two waveguide filters ([21], [36]), one operating at WR-3 band (220-325 GHz) the other at WR-1.5 band (500-750 GHz), both fabricated using the SU-8 photolithography process, will be given as examples.

2.1 Design of WR-3 band filter

The first device, shown in Fig. 1, is a 5th order asymmetrical capacitive iris coupled WR-3 bandpass filter. The filter is designed to have a centre frequency of 300 GHz and a fractional equal-ripple bandwidth of 9%. The dimensions of the filter are obtained by following an approach as described in [37].

A layering technique is utilised to accommodate the design for the SU-8 process. As shown in Fig. 1, the filter is divided into four layers, so that each layer can be fabricated by the SU-8 photolithography process. The entire filter can be finally constructed by assembling the metal coated SU-8 layers together. The photolithography process does not allow structures with variable depths in one layer, but does have good vertical sidewalls (<1° taper angle [26]). In order to simplify the fabrication, all the layers are usually designed to have the same thickness, so that they can be made by photolithography using a single mask. The waveguide filter is made with capacitive irises to be consistent with the layered structure, and they are used to provide the required external and inner couplings between resonators. As seen in Fig. 1, these irises are placed asymmetrically; since compared with the symmetrical ones, for the same coupling coefficient, the asymmetrical iris has a larger gap [25]. The iris for couplings between resonators 2 and 3, or 3 and 4, has the smallest gap of around 91 μm. This corresponds to an aspect ratio of nearly 5:1, and is readily achievable for SU-8 process, but would be very challenging for CNC machining.

The technique means that the devices are formed with several SU-8 layers. An immediate problem is localized air gaps between different layers. The filter in Fig. 1 is split in the E-plane in order to minimize insertion loss due to such air gaps. As mentioned before, the joints on the middle of the broadside wall are not in the path of any surface current flow, and therefore have little impact on the insertion loss. Joints between layers 1 and 2 can be eliminated, as they can be joined together through a two-layer SU-8 process (to be described in Section 2.3). This prevents the joints that would have an adverse impact on performance. Although the joints can be a problem, careful attention to the flatness of the device and bonding the layers has produced good results, as demonstrated by (i) WR-3 and WR-5 waveguides [29] (based on five SU-8 layers) where current path is split; and (ii) a WR-1.5 filter as described in the section below. This is expected to improve as the SU-8 process matures further.

2.2 Design of WR-1.5 band filter

The second example is a 3rd order WR-1.5 band waveguide filter, shown in Fig. 2 (a)-(c). It is designed to

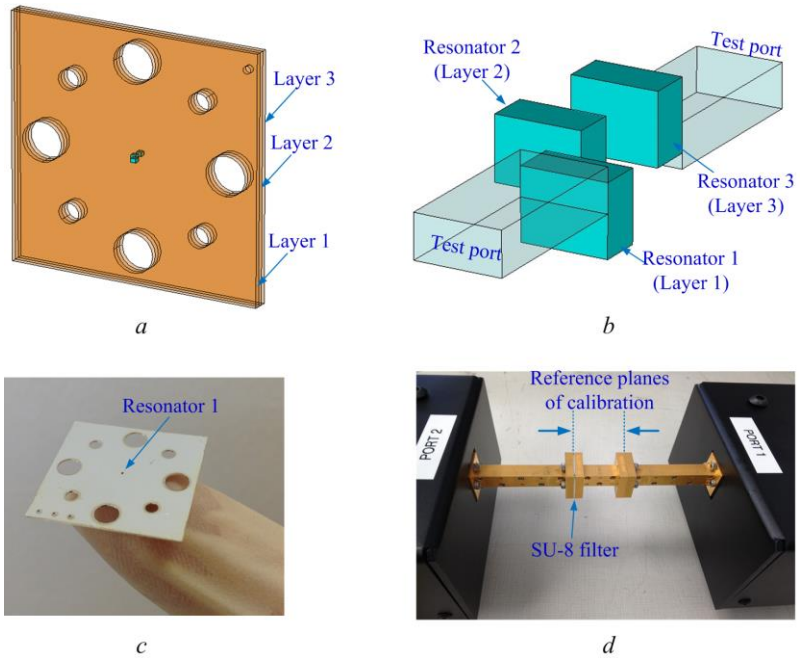

Fig. 2. *WR-1.5 waveguide filter consisting of three SU-8 layers with an identical thickness of 191 µm. [36]*
(a) Illustration of the filter which is based on three silver coated SU-8 shims.
(b) Detail of the filter structure corresponding to the part in (a).
(c) Photograph of SU-8 Layer 1 which is fully coated with silver.
(d) Measurement setup for the SU-8 filter.

have an equal ripple bandwidth of 5% centred at 650 GHz. The filter is designed by following the approach in [37]. Different to conventional filters based on inductive/capacitive irises, this filter is based on three resonators which are offset and uses the relative shift in positions of resonators to alter couplings. The first and third resonators are connected directly to the test ports, eliminating the need for SU-8 waveguide connections at either end of the filter. This reduces the insertion loss of the whole filter.

As shown in Fig. 2 (a), the filter is constructed from three SU-8 thin shims, with each shim containing only one resonator. This leads to significant reduction in the geometric complexity of the whole device, and yields improved reliability and performance. Such a filter structure is ideally suited to the layered SU-8 micromachining process. CNC machining is unable to produce this type of filter structure from a metal block, mainly because the milling tool cannot reach the central segment on layer 2. The layers are also too thin to be machined separately on a CNC machine. The measurement results of this device are given in Section 2.4.

2.3 SU-8 fabrication process

Both SU-8 single layer lithography and SU-8 two-layer lithography processes have been developed and utilised to produce waveguide devices. The former mainly concerns designs with relatively simple geometries (e.g. WR-1.5 filter in Section 2.2), and the latter could be used for more complex designs. Fig. 3 shows the key steps for SU-8 single-layer and two-layer processing. Initially, liquid SU-8 is spun onto a 4 inch diameter silicon wafer, prebaking the SU-8 to solidify it enough to be able to UV expose the required pattern through a mask, i.e. steps (a) and (b) in Fig. 3. For the single layer process, the structure is baked after exposure to form cross-link, and then released from the silicon wafer by development, i.e. step (c) in Fig. 3. To go through the full two-layer process, the first SU-8 layer would be subject to a post exposure bake at low temperature to form weak crosslink, before the second SU-8 layer is spin coated on top, see steps (d)-(e). Similarly, an exposure of UV light, post-exposure bake and development are carried out, i.e. steps (f)-(g). The final product is a fully cross-linked and joined two layered SU-8 structure, without internal joints.

The SU-8 structures are usually metallised all around with 2 μm thick silver or gold layer using evaporation. Prior to evaporation, a 5 *n*m thick chromium layer is evaporated on the SU-8 structure for improved adhesion. Finally, several layers of metal coated SU-8 are assembled together using precision alignment pins. More detailed discussion about the fabrication process can be found in [21] and [24].

It is worth pointing out that the single layer process does not permit isolated islands (i.e. features that can't stand alone without support). The two-layer process lifts this restriction and allows standalone regions on the top layer. This enables realisation of some complex designs, e.g. a WR-3 band 8th order cross-coupled dual-band filter [21]. In addition, the two-layer process is desirable as it can eliminate the inner joints between layers and avoid localized air gaps. This could particularly benefit large size SU-8 designs, where localized air gaps usually exist due to thickness non-uniformity across the whole layer (usually on the order of several micrometers).

2.4 Measurement and discussions

The assembly and measurement of micromachined waveguide devices is challenging due to the difficulties in (i) precise alignment between layers of micromachined devices and (ii) accurate connection to the standard waveguide flange of the measurement equipment. Apart from the efforts of developing the micromachining techniques,

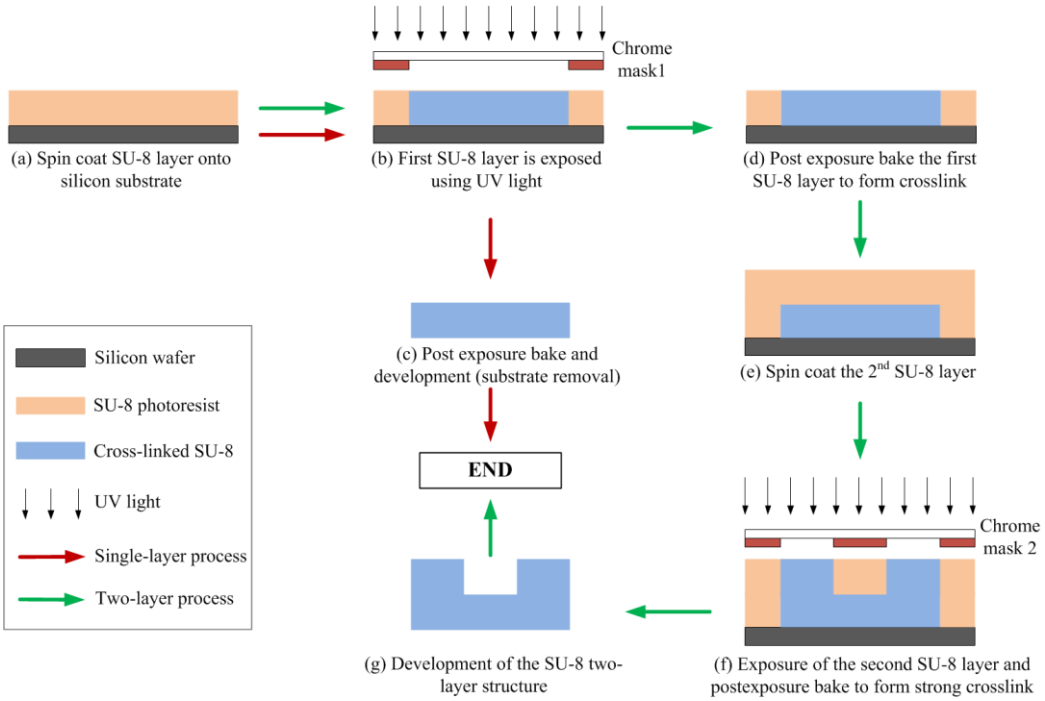

Fig. 3. *Schematic of the key steps in the SU-8 single and two-layer processes.*

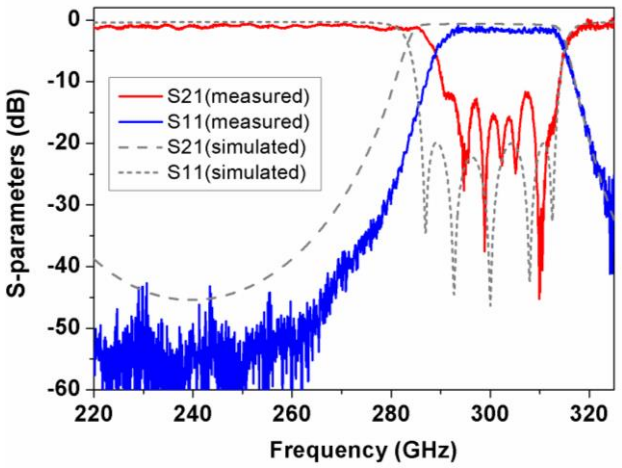

Fig. 4. *Measurement and simulation results of the WR-3 band filter in Fig.1. [21]*

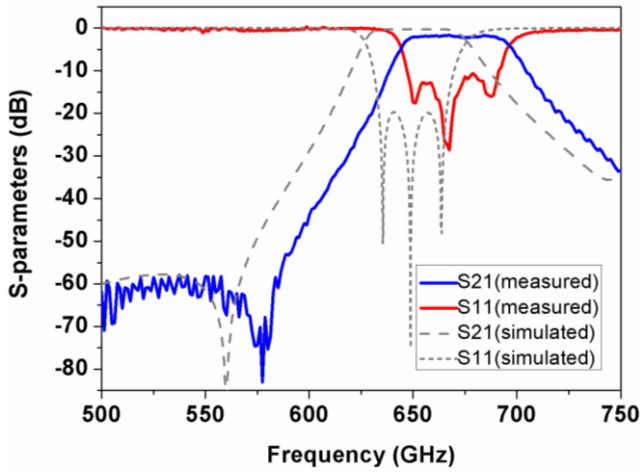

Fig. 5. *Measurement and simulation results of the WR-1.5 band filter in Fig. 2. [36].*

researchers have also been investigating reliable and accurate assembly and measurement techniques for micromachined devices. In [20], a novel silicon micromachined compression pin is reported and it is capable of providing a wafer to wafer alignment accuracy to less than 1 μm. This is demonstrated by excellent measured performance of WR-1.5 band waveguides and 3 dB coupler, all of which are assembled using this specialised pin. In [38], a novel WR-3 band waveguide flange based on bandgap structures is presented to ease the requirement of intimate contact between micromachined circuits and test equipment. This new flange permits a small gap (as wide as 50 μm) at the interface and therefore enables contactless and fast measurements. The concept is validated using a 1 inch long WR-3 waveguide with good measured performance.

In general there are two calibrated measurement methods for evaluation of SU-8 devices. The first one uses a precision machined metal block constructed from two separate pieces in which the SU-8 circuit is sandwiched between. The second method integrates the flanges with the circuit and patterns the flanges directly during SU-8 processing. Both of these techniques are explained in detail in [39]. Here, the WR-3 band filter has used the former and the WR-1.5 band filter the latter technique for measurement.

Fig. 4 shows the measured performance of the WR-3 band filter. There is a narrowing of the -3 dB bandwidth, from 10% (simulation) to 8% (measurement). It is believed the difference is attributed to the inaccuracies in critical dimensions as well as around 5% narrower iris gaps. Both problems can be corrected by fabricating another device with modified dimensions (i.e. by adjusting the dimensions on the mask). This is feasible as the SU-8 process is photolithography based and therefore offers excellent repeatability of devices produced in different batches [40]. The filter is measured to have an insertion loss of 1.6 dB and a return loss of better than 10 dB across the passband [21].

Fig. 2 (d) shows the test setup of the WR-1.5 filter. These SU-8 layers are delicate owing to their thinness (191 μm), and are therefore carefully mounted onto a separate metal through waveguide section first, and then inserted between the two ports to carry out the measurement. The measurement results of the SU-8 filter together with the 1 inch long waveguide section are shown in Fig. 5. The filter is measured to have a -3 dB bandwidth of 53.7 GHz at a centre frequency of 671 GHz. The median insertion loss in the passband is measured to be 1.75 dB and the measured return loss is better than 11 dB across the whole passband. After removing the effect of the waveguide section, the passband loss from the filter is calculated to be around 0.65 dB, which is only 0.37 dB higher than the expected value obtained from simulation using silver. The centre frequency is shifted upwards and this is attributed to dimensional inaccuracies [36].

Both SU-8 made filters have been tested to have a good performance. As with other micromachining techniques, the SU-8 process also has intrinsic limitations. The three major constraints listed below need to be taken into consideration when designing SU-8 devices.

(1) SU-8 can be used to pattern structures with very high aspect ratios (>20:1). However, in the designs the aspect ratios should be made much lower than 20:1 (ideally within 5:1). This limitation is imposed by the metal coating using vacuum deposition process, which has difficulty to coat deep structures. Metal coating using sputtering may overcome this problem, since it is a non-directional deposition technique. Conventional high precision CNC machining offers an aspect ratio no greater than 3:1, and therefore the SU-8 process is still superior to CNC from this perspective.

(2) The lateral dimensions of SU-8 structures are dependent on the mask which is intrinsically high accuracy. The waveguide circuits implemented to date demonstrate a lateral dimensional accuracy smaller than 2 μm [33]. The thickness of SU-8 layers is dependent upon the spinning and processing of the SU-8 resist, and is within ± 10 μm. It can be improved through an additional step of polishing. As an alternative to improvement on process, the devices can also be made accurately by iterations, i.e. making the devices again with modified dimensions which take fabrication inaccuracies into account.

(3) The SU-8 process is not a desired choice for devices operating with a very high power level, at a high temperature or requiring a high thermal stability. Cross-linked (or exposed) SU-8 has a glass transition temperature of > 200 °C [41], and this indicates the maximum operating temperature of circuits formed of SU-8. Note that the

operating temperature is also limited by difference of coefficient of thermal expansion (CTE) between SU-8 and the coated metal. The former has a CTE of around 52×10^{-6}/K [41] and the latter 18×10^{-6}/K (in case of silver). High operating temperature results into difference in expansions, and yields considerable tension between SU-8 and metal coating. In the scenario where a high thermal stability is demanded, the SU-8 photolithography process can be used together with electroplating to construct all-copper based devices [9]. This combined process, which is effectively metal electroforming, uses SU-8 as a mould to form the desired copper structures. Such all-copper devices have excellent thermal stability, and high dimensional accuracy which is transferred from the SU-8 features patterned using lithography process.

3. Laser micromachining

Laser micromachining is a promising alternative for the fabrication of a wide range of micro-components, and has some very attractive advantages in comparison to existing techniques. Current lasers can produce features as small as 10-20 μm and are therefore are an excellent choice for the small to medium batch size production of terahertz waveguide devices. Laser micromachining is a non-contact process, with relatively high accuracy and repeatability at the micro scale and can be used for structuring a wide range of materials and for producing complex features with varying depths.

Compared to high precision CNC milling, laser micromachining can in principle achieve smaller feature sizes with comparable dimensional and geometrical accuracy. Additionally, as laser micromachining is a non-contact process, there is no tool-wear or generation of defects and cracks due to mechanical stresses. The previous section shows that the SU-8 process can be employed as a feasible alternative to high precision CNC milling in terms of accuracy and cost. The main disadvantage of the SU-8 process is that SU-8 is a polymer based photoresist with relatively poor thermal stability. Laser micromachining can produce terahertz circuits on metal substrates directly and is therefore an ideal choice to complement the SU-8 process. In addition, laser micromachining is capable of producing waveguide structures with varying depths (or heights) from one workpiece, and therefore eliminates the need for splitting the device into several layers and aligning them with a high accuracy.

Laser micromachining has already been utilised for the production of various optical or quasi-optical components, such as two terahertz mesh filters; one machined from stainless steel and the other molybdenum [42]. However, it is rarely employed to produce submillimeter-wave waveguide components, except for a 2-THz corrugated horn antenna machined from silicon [43]. This antenna is machined from two silicon substrates, coated with gold via a sputtering process, and finally assembled. Here, we will discuss a proof-of-concept demonstration of a W-band waveguide filter [5], which has been specially designed to take full advantage of the flexibility offered by laser micromachining.

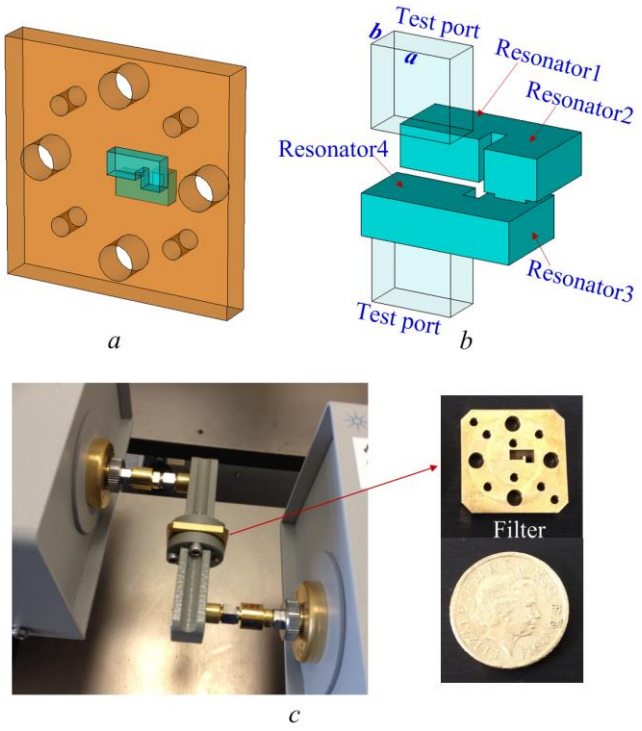

Fig. 6. *Laser machined W-band filter [5].*
(a) Illustration of the whole filter based on a single piece.
(b) Detail of the filter structure corresponding to the part in (a).
(c) Photograph of filter and test setup.

3.1. Design of W-band filter

A 4th order W-band filter, designed for laser micromachining is shown in Fig. 6. The filter is designed with a centre frequency of 100 GHz and an equal ripple bandwidth of 4%. Similar to the WR-1.5 filter shown in Fig. 2, resonators 1 and 4 are connected directly to the test ports and the external couplings are controlled by shifting of their relative positions. Couplings between resonators are provided by inductive irises and slots. A detailed description of the filter design can be found in [5].

Laser processing is a non-contact process, and this enables processing from both sides of the sample. The unique structure of the filter allows such processing in a single setup, i.e. the entire filter structure can be made all at once. There is no need to mount/dismount the device several times, and this reduces the setting up and machining time as well as ensures good alignment accuracy between resonators on both sides. Furthermore, the whole filter can be produced into a standalone component, instead of assembling from several pieces. This yields an improved performance and reliability. CNC machining may struggle to accomplish similar double-side operations, mainly due to the mechanical stress generated during milling.

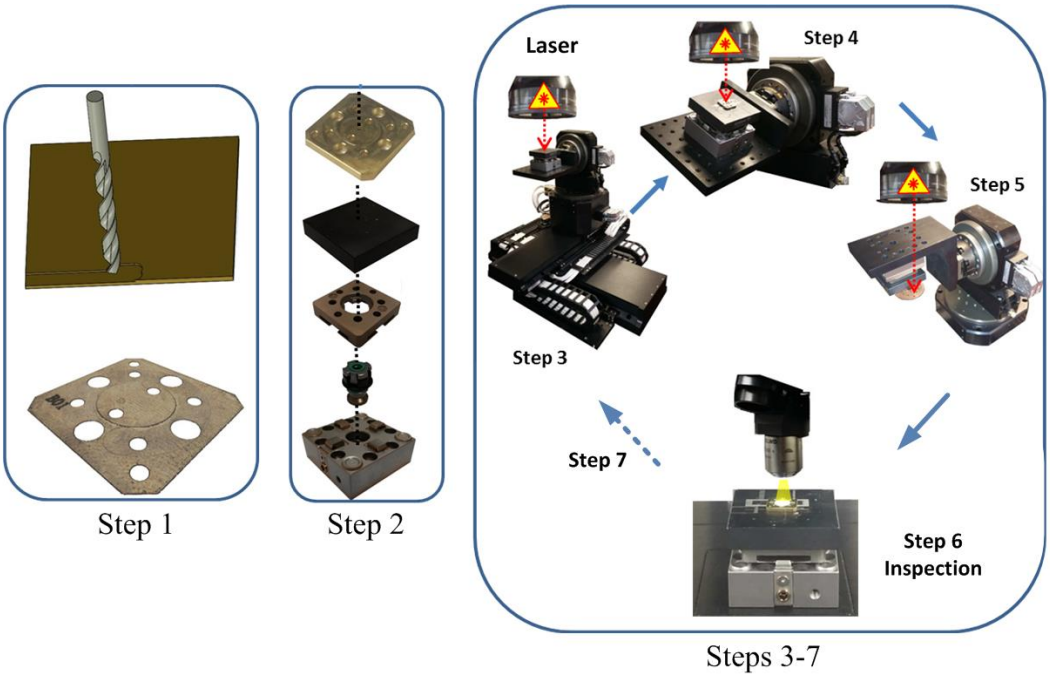

Fig. 7. *Diagram illustrating key steps of laser micro-machining process. [5]*

3.2 Laser micromachining process

Laser micromachining is only viable when small structures are to be machined because of the relatively low removal rates in comparison to conventional milling. Furthermore, the laser machined structures generally have tapered sidewalls, which can have a significant impact on the performance of terahertz devices if the taper angle is not taken into account during design. Ideally, waveguides need to have perfect rectangular cross sections in order to achieve good match between devices mounted together [22]. These problems have to be overcome in order to make laser micromachining feasible for producing terahertz devices.

A multi-stage processing chain, as shown in Fig. 7, is proposed to address the first problem. This process chain integrates conventional standard CNC milling with laser micro-machining. Alignment and fixing holes for connection to flanges, are produced using conventional milling in order to reach a higher material removal rate. Laser micromachining is utilised to produce the resonators and coupling irises with a higher dimensional accuracy. The problem of taper angle on sidewalls can be overcome by employing an optimised laser beam path [5].

The laser micromachining is carried out on a platform which integrates a 5 W laser source provided by Amplitude Systems. This pulsed laser source operates at a wavelength of 1030 *n*m with a highest pulse repetition rate of 500 kHz. The beam spot diameter, measured at the focal plane, is 45 μm, and this can be adjusted using an additional lens. Fig. 7 shows the key fabrication steps of the laser machining process. These steps are also summarized as follows [5]:

(1) Produce the alignment and fixing holes on a brass plate with the desired thickness on a conventional standard CNC machine;

(2) Mount the brass plate to a modular workpiece for the follow-up double side laser processing;

(3) Fabricate filter features on one side of the brass plate using laser micromachining;

(4) Make use of multi-axis machining and rotary stages to reach and process tapered sidewalls. Detailed operations are based on calculations and results from experimental trials. After this step, nearly vertical sidewalls (taper angle < 0.5°) are usually obtained;

(5) Reposition of the workpiece which holds the brass device at 180°, with the help of rotary stages, in order to gain access to the opposite side of the waveguide device for repetition of Steps (3)-(4);

(6) Inspect the produced filter on a high resolution microscope to identify deviations of dimensions compared with nominal ones;

(7) Final small operations to resolve deviations found in Step (6), which ends up with the final filter.

The double-side processing mentioned before is implemented at Step (5). This step requires repositioning of the workpiece which involves rotations of the stage, and a well-established process provides a precise repositioning, with an evaluated accuracy and repeatability better than 10 μm [44]. Additionally, Step (7) can be eliminated from the process chain through extensive process development, e.g. optimisation of laser processing parameters and settings. More details about the laser machining process can be found from [5] and [44-45].

Table 1 Comparison of micromachining techniques

Techniques	Achievable aspect ratio	Dimensional accuracy	Surface roughness	Batch / Serial fabrication	Ref.
3D SLA printing	>100:1	<25 μm	1 μm (R_{RMS})	Serial	[12]
3D SLS printing	>15:1	<100 μm	6 μm (R_a)	Serial	[13]
CNC machining	>5:1	<2 μm	75 *n*m (R_a)	Serial	[7]
DRIE process	>30:1	<2 μm	100 *n*m (R_{RMS})	Batch	[19]
Electroforming	>20:1	<1 μm	300 *n*m (R_{RMS})	Batch	[8]
Hot embossing	>7:1	<25 μm	135 *n*m (R_{RMS})	Batch	[46-47]
SU-8 process	>20:1	<2 μm	40-50 *n*m (R_{RMS})	Batch	[33]
Laser machining	>3:1	<10 μm	1.5 μm (R_a)	Serial	[44-45]

3.3 Measurement and discussions

Fig. 6 (c) shows the test setup of the laser machined W-band filter. During measurements, the filter is placed between the flanges of the waveguide connected network analyser. The measurement performance of the filter is shown in Fig. 8. The measured insertion loss and return loss across the passband are 0.65 dB, and 15 dB, respectively. The measured insertion loss is close to predicated value of 0.3 dB obtained from simulations with brass. Overall the measurement agrees well with simulations.

From this example, it is clear that laser micromachining is a viable option for high frequency filters. Two factors affecting the performance are identified and discussed below.

(1) In this example the surface roughness of laser processed area is on the order of 1.25 μm. This results in an additional loss of 0.22 dB [5], which is responsible for a large portion of the difference between the measured and simulated passband loss. Surface roughness can be reduced through further optimisation of laser parameters settings, e.g. pulse repetition rates, beam spot diameters and the hatch angle between laser machining layers [45]. Note that the optimal laser parameters vary with different materials under processing. For silicon, the optimised process can achieve a roughness on the order of 200 *n*m [43]. This could be reduced further to under 25 *n*m using standard chemical polishing [43].

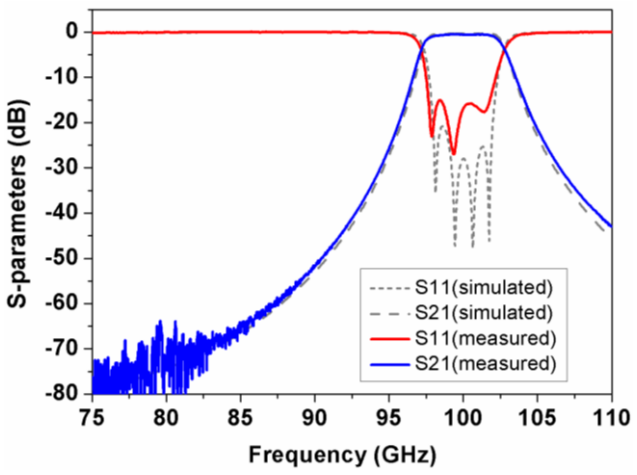

Fig. 8. *Measurement and simulation results of the laser machined W-band filter. [5]*

(2) The machined W-band filter has a measured dimensional accuracy of around 10 μm. The dimensional accuracy greatly depends on the process parameter settings used for production and still has room to improve through further optimisation.

4. Conclusion

This paper has reviewed micromachining techniques for the fabrication of submillimeter-wave and terahertz waveguide devices, with a particular emphasis on waveguide filters. The SU-8 and laser micromachining processes have been utilised to produce a series of waveguide devices operating at frequencies from around 60 GHz to 700 GHz. It is envisaged that waveguide devices operating at frequencies higher than 700 GHz are to be fabricated using these two micromachining techniques in the future. In this paper, both techniques have been described with examples of submillimeter-wave waveguide filters.

Table-1 shows a comparison of micromachining techniques. Aspect ratio shown in the table indicates the capability of the process itself, and in practice the maximum aspect ratio of the device might be lower due to the limitation of other factors (e.g. plating process required for SLA printing, etc). Table-2 summarises the recently published waveguide filters operating in the frequency range from W-band to WR-1 band. It can be observed that both the SU-8 process and laser micromachining can produce waveguide filters with comparable performance to those made by other conventional techniques such as high precision CNC machining and DRIE process. Although the laser micromachining process is relatively new, the expectation of it producing viable terahertz circuits is high. The potential of both techniques for the production of millimetre-wave and terahertz waveguide components has been demonstrated.

5. Acknowledgments

This work was supported by the UK Engineering and Physical Science Research Council (EPSRC) under Contract EP/M016269/1.

Table 2 Comparison of published waveguide filters operating in the frequency range from W-band to WR-1 band

Waveguide band	f_o (GHz)	*FBW*	Filter type	*n*	*IL* (dB)	*RL* (dB)	Manufacturing techniques	Split block	Ref. (year)
WR-10	100	10%	Extracted pole filter with elliptical response	4	0.6	>18	CNC milling	no	[1] (2012)
WR-10	92.6	4.53%	Chebyshev filter	4	0.5	>14	CNC milling	yes	[2] (2014)
WR-10	88.47	9.7%	Chebyshev filter	4	1	>15	SU-8 process	yes	[25] (2011)
WR-10	102	5%	Extracted pole filter with Pseudo-Elliptical response	4	1.2	>10	SU-8 process	no	[26] (2012)
WR-10	107.2	6.34%	Chebyshev filter	6	0.95	>11	3-D printing	no	[11] (2015)
WR-10	92.45	4.83%	Chebyshev filter	3	1.2	>10	DRIE	no	[14] (2006)
WR-10	95	3.68%	Chebyshev filter	5	3.49	>18	Micro-hot embossing	no	[23] (2005)
WR-10	100	4%	Chebyshev filter	4	0.65	>15	Laser micromachining	no	[5] (2016)
WR-10	87.5	11.5%	Chebyshev filter	4	0.4	>18	3-D printing	no	[5] (2016)
WR-6	139.2	8.3%	Chebyshev filter	7	1	>16.4	CNC milling	yes	[3] (2012)
WR-3	255	11.76%	Chebyshev filter	5	3.9	>15	CNC milling	yes	[4] (2015)
WR-3	256	9.8%	Quasi-elliptical filter	4	0.5	>15	CNC milling	no	[48] (2017)
WR-3	300	8%	Chebyshev filter	5	1	>10	SU-8 process	yes	[21] (2012)
WR-2.2	395.05	7.52%	Dual mode filter with elliptical response	4	2.84	>16	DRIE	no	[15] (2015)
WR-2.2	385	3.9%	Chebyshev filter	2	2.7	>7	DRIE	no	[16] (2012)
WR-1.5	570	8.77%	Chebyshev filter	3	0.9	>10	DRIE	no	[17] (2012)
WR-1.5	640	10%	Chebyshev filter	5	1	>10	DRIE	yes	[18] (2013)
WR-1.5	671	8%	Chebyshev filter	3	0.65	>11	SU-8 process	no	[36] (2013)
WR-1	982	13.1%	Chebyshev filter	5	2.5	>14	DRIE	–	[19] (2014)
WR-1	1017	2.2%	Dual mode filter with elliptical response	4	2.9	>15	DRIE	no	[49] (2016)

Note: f_o: center frequency of the filter; *FBW*: fractional bandwidth; *n*: filter order; *IL*: passband insertion loss; *RL*: passband return loss

6. References

[1] Leal-Sevillano, C.A., Montejo-Garai, J.R., Ruiz-Cruz, J.A., *et al.*: 'Low-loss elliptical response filter at 100 GHz', IEEE Microw. Wireless Compon. Lett., 2012, **22**, (9), pp.459-461

[2] Liao, X., Wan, L., Yin, Y., *et al.*: 'W-band low-loss bandpass filter using rectangular resonant cavities', IET Microw. Antennas Propag., 2014, **8**, (15), pp.1440-1444

[3] Wang, C., Lu, B., Liu, J., *et al.*: '140 GHz waveguide H ladder bandpass filter'. Int. Conf. Microw. Millimeter Wave Techn, Shenzhen, China, May 2012, pp. 1-4

[4] Zhuang, J., Hong, W., Hao, Z.: 'Design and analysis of a terahertz bandpass filter', Int. Wireless Symposium (IWS), Shenzhen, China, 2015, pp. 1-4

[5] Shang, X., Penchev, P., Guo, C., *et al.*: 'W-band waveguide filters fabricated by laser micromachining and 3-D printing', IEEE Trans. Microw. Theory Tech., 2016, **64**, (8), pp. 2572-2580

[6] Leal-Sevillano, C.A., Cooper, K.B., Decrossas, E., *et al.*: 'Compact duplexing for a 680-GHz radar using a waveguide orthomode transducer', IEEE Trans. Microw. Theory Tech., 2014, **62**, (11), pp. 2833-2842

[7] Groppi, C.E., Love, B., Underhill, M., *et al.*: 'Automated CNC micromachining for integrated THz waveguide circuits'. 21st International Symp. Space THz Technology, Oxford, UK, March 2010, pp. 338-341

[8] Mena, F.P., Kooi, J., Baryshev, A.M., *et al.*: 'RF performance of a 600-720 GHz sideband-separating mixer with all-copper micromachined waveguide mixer block', 19th International Symp. Space THz Technology, Groningen, Netherlands, April 2008, pp. 90-92

[9] Pavolotsky, A., Meledin, D., Risacher, C., *et al.*: 'Micromachining approach in fabricating of THz waveguide components', Microelectronics Journal, 2005, **36**, (7), pp. 683-686

[10] Guo, C., Shang, X., Lancaster, M. J., *et al*: 'A 3-D printed lightweight X-band waveguide filter based on spherical resonator', IEEE Microw. Wireless Compon. Lett., 2015, **25**, (7), pp.442-444

[11] D'Auria, M., Otter, W. J., Hazell, J., *et al.*: '3-D printed metal-pipe rectangular waveguides', IEEE Trans. Compon. Packag. Manuf. Techn., 2015, **5**, (9), pp.1339-1349

[12] 'Swissto12, Lausanne, Switzerland', http://www.swissto12.com, accessed October 2016

[13] Zhang, B., Zirath H.: '3D printed iris bandpass filters for millimetre-wave applications', Electronics Letters., 2015, **51**, (22), pp. 1791-1793

[14] Li, Y., Kirby, P.L., Papapolymerou, J.: 'Silicon micromachined W-band bandpass filter using DRIE technique'. 36th European Microwave Conf., Manchester, UK, Sept 2006, pp. 1271–1273

[15] Zhuang, J.X., Hao, Z.C., Hong, W.: 'Silicon micromachined terahertz bandpass filter with elliptic cavities', IEEE Trans. Terahertz. Science and Technology., 2015, **5**, (6), pp. 1040-1047

[16] Hu, J., Xie, S., Zhang, Y., 'Micromachined terahertz rectangular waveguide bandpass filter on silicon-substrate', IEEE Microw. Wireless Compon. Lett., 2012, **22**, (12), pp. 636-638

[17] Leong, K.M.K.H., Hennig, K., Zhang, C., *et al.*: 'WR1.5 silicon micromachined waveguide components and active circuit integration methodology', IEEE Trans. Microw. Theory Tech., 2015, **60**, (4), pp. 998-1005

[18] Leal-Sevillano, C.A., Reck, T.J., Jung-Kubiak, C., *et al.*: 'Silicon micromachined canonical E-plane and H-plane bandpass filters at the terahertz band', IEEE Microw. Wireless Compon. Lett., 2013, **23**, (6), pp. 288-290

[19] Reck, T., Jung-Kubiak, C., Leal-Sevillano, C., *et al.*: 'Silicon micromachined waveguide components at 0.75 to 1.1 THz'. 39th Int. Conf. Infrared, Millimeter, and Terahertz waves (IRMMW-THz), Tucson, AZ, 2014, pp. 1-2

[20] Reck, T. J., Jung-Kubiak, C., Gill, J., *et al*: 'Measurement of silicon micromachined waveguide components at 500-750 GHz', IEEE Trans. Terahertz. Science and Technology, 2014, **4**, (1), pp. 33-38

[21] Shang, X., Ke, M., Wang, Y., *et al.*: 'WR-3 band waveguide and filters fabricated using SU8 photoresist micromachining technology', IEEE Trans. Terahertz. Science and Technology., 2012, **2**, (6), pp. 629-637

[22] Jung-Kubiak, C., Reck, T. J., Siles, J. V., *et al.*: 'A multistep DRIE process for complex terahertz waveguide components', IEEE Trans. Microw. Theory Tech., 2016, **6**, (5), pp. 690-695

[23] Sammoura, F., Cai, Y., Chi, C. Y., Hirano, T., Lin, L., Chiao, J. C.: 'A micromachined W-band iris filter', 13th Int. Conf. Solid-state Sensors, Actuators and Microsystems, Seoul, South Korea, June 2005, pp. 1067-1070

[24] Tian, Y., Shang, X., Wang, Y., *et al.*: 'Investigation of SU8 as a structural material for fabricating passive millimeter-wave and terahertz components', J. Micro/Nanolith. MEMS MOEMS., 2015, **14**, (4), 044507

[25] Shang, X., Ke, M., Wang, Y., *et al.*: 'Micromachined W-band waveguide and filter with two embedded H-plane bends', IET Microw. Antennas Propag., 2011, **5**, (3), pp.334-339

[26] Leal-Sevillano, C. A., Montejo-Garai, J. R., Ke, M., *et al.*: 'A pseudo-elliptical response filter at W-band fabricated with thick SU-8 photo-resist technology', IEEE Microw. Wireless Compon. Lett., 2012, **22**, (3), pp.105-107

[27] Wang, Y., Ke, M., Lancaster, M. J.: 'Micromachined 60 GHz air-filled interdigital bandpass filter', Int. Workshop on Microwave Filters., Toulouse, France, November 2009, pp.1-5

[28] Wang, Y., Yang, B., Tian, Y., *et al.*: 'Micromachined thick mesh filters for millimeter-wave and terahertz applications', IEEE Trans. Terahertz. Science and Technology., 2014, **4**, (2), pp. 247-253

[29] Glynn, D., He, T., Powell, J. *et al*: 'Submillimetre rectangular waveguides based on SU-8 photoresist micromachining technology', 46th European Microwave Conference, London, UK, October 2016, pp. 417-420

[30] Smith, C.H., Sklavonuos, A., Barker, N.S.: 'SU-8 micromachining of millimeter and submillimeter waveguide circuits', IEEE MTT-S International Microwave Symposium Digest, Boston, USA, June 2009, pp. 961-964.

[31] Murad, N.A., Lancaster, M.J., Wang, Y., Ke, M.L.: 'Micromachined millimeter-wave Butler matrix with a patch antenna array', Mediterrannean Microwave Symposium (MMS), Tangiers, Morocco, November 2009, pp. 1-4

[32] Leal-Sevillano, C.A., Tian, Y., Lancaster, M.J., *et al.*: 'A micromachined dual-band orthomode transducer', IEEE Trans. Microw. Theory Tech., 2014, **62**, (1), pp. 55-63

[33] Wang, Y., Ke, M., Lancaster M.J., *et al*: 'Micromachined 300GHz SU-8-based slotted waveguide

antenna', IEEE Antennas Wireless Propga. Lett., 2011, **10**, pp. 573-576
[34] Murad, N.A., Lancaster, M.J., Gardner, P., *et al*.: 'Micromachined H-plane horn antenna manufactured using thick SU-8 photoresist', Electronics Letters., May 2010, **46,** (11), pp. 743-745
[35] Konstantinidis, K., Feresidis, A.P., Tian, Y., *et al*.: 'Micromachined terahertz fabry-perot cavity highly directive antennas', IET Microw. Antennas Propag., 2015, **9**, (13), pp. 1436-1443
[36] Shang, X., Tian, Y., Lancaster, M.J., *et al*.: 'A SU8 micromachined WR-1.5 band waveguide filter', IEEE Microw. Wireless Compon. Lett., 2013, **23**, (6), pp. 300-302
[37] Hong, J. -S., Lancaster, M.J.: 'Microstrip filters for RF/microwave applications' (John Wiley &Sons, 2001)
[38] Rahiminejad, S., Pucci, E., Vassilev, V., *et al*: 'Polymer gap adapter for contactless, robust, and fast measurements at 220-325GHz', Journal of Microelectromechanical Systems, 2016, **25**, (1), pp. 160-169
[39] Shang, X., Lancaster, M.J., Ke, M., *et al*: 'Measurements of micromachined submillimeter waveguide circuits', 76th ARFTG Microwave Measurement Symposium, Florida, USA, 30 Nov. – 3 Dec. 2010, pp. 1-4
[40] Tian, Y., Shang, X., Lancaster, M. J.: 'Fabrication of multi-layered SU8 structure for terahertz waveguide with ultralow transmission loss', J. Micro/Nanolith. MEMS MOEMS, 2014, **13**, (1), pp. 013002-1
[41] Mitra, S. K., Chakraborty, S.: 'Microfluidics and nanofluidics handbook: fabrication, implementation and applications' (CRC Press, April 2016)
[42] Voisiat, B., Bičiūnas, A., Kašalynas, I., *et al*.: 'Band-pass filters for THz spectral range fabricated by laser ablation', Appl. Phys. A, 2011, **104**, (3), pp. 953-958
[43] Walker, C.K., Knoepfle, H., Capara, J., *et al*.: 'Laser micromachining of silicon: a new technique for fabricating high quality terahertz waveguide components', Proc. 8th Int. Symp. Space THz Technolo., Cambridge, MA, USA, Mar 1997, pp. 358-376
[44] Penchev, P., Dimov, S., Bhaduri, D., *et al*: 'Generic integration tools for reconfigurable laser micromachining systems', J. Manuf. Syst., 2016, **38**, pp. 27-45
[45] Penchev, P., Shang, X., Dimov, S., *et al*.: 'Novel manufacturing route for scale up production of terahertz technology devices', ASME Journal of Micro- and Nano-Manufacturing, 2016, **4**, pp. 021002-021002-14
[46] Sammoura, F., Su, Y. C., Cai, Y., *et al*: 'Plastic 95-GHz rectangular waveguides by micro molding technologies', Sensors and Actuators A: Physical, 2006, **127**, (2), pp. 270-275
[47] Becker, H., Heim, U.: 'Hot embossing as a method for fabrication of polymer high aspect ratio structures', Sensors and Actuators A: Physical, 2000, **83**, (1), pp. 130-135
[48] Ding, J. Q., Shi, S. C., Zhou, K., *et al*: 'WR-3 band quasi-elliptical waveguide filters using higher order mode resonances', IEEE Trans. Terahertz Science and Technology, 2017, **7**, (3), pp. 302-309
[49] Liu, S., Hu, J., Zhang, Y., Zheng, *et al*.: '1 THz micromachined waveguide band-pass filter', Journal Infrared Milli. Terahz Waves, 2016, **37**, pp. 435-447